Theoretical and Single-Crystal ESR Study of the Structure and Dissociation of a $R_2PCl^{\bullet -}$ Radical Anion

Maria Cattani-Lorente,[†] Michel Geoffroy,*[†] Shuddhodan P. Mishra,[†] Jacques Weber,[‡] and Gerald Bernardinelli[⊥]

Contribution from the Department of Chemistry, University of Geneva, 1211 Geneva 4, Switzerland. *Received May 1, 1986*

Abstract: Experimental information about the structure of a $R_2PCl^{\bullet -}$ ion is obtained from the ESR study of an X-irradiated single crystal of 1,2-phenylenephosphorochloridite. The crystal structure of this compound is determined and is used to discuss the hyperfine interaction with ^{31}P and ^{35}Cl. The unpaired electron is strongly localized in a P–Cl σ^*-orbital and the radical anion is shown to thermally dissociate into a phosphinyl radical and a Cl^- ion. Ab initio calculations show that the geometry of $PCl_3^{\bullet -}$ is of the planar T-shape type whereas $H_2PCl^{\bullet -}$ adopts a pyramidal structure, which is in good agreement with the experimental results. The theoretical dissociation energy $PH_2Cl^- \rightarrow \dot{P}H_2 + Cl^-$ is calculated to be ~7 kcal.

Electron capture by phosphorus-containing molecules is well documented for tetra- and pentacoordinated species: the resulting phosphoranyl radicals[1] ($\dot{P}R_4$) and phosphorane anions[2] ($PR_5^{\bullet -}$) have been identified by ESR and their structures have been intensively investigated by ab initio[3] and semiempirical[4,5] quantum chemical methods. However, radical anions derived from tricoordinated phosphorus species are considerably less known and only $(MeO)_3P^{\bullet -}$ has been tentatively identified in irradiated frozen solutions of trimethyl phosphite.[6]

Various structures have been proposed for 27 electron radicals bearing a lone pair: the trigonal bipyramid[6] a, the T-shape[7] b, the planar structure[8] c, and the σ^* structure[9] d.

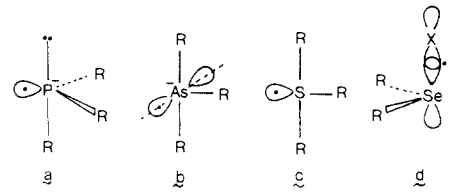

a b c d

In the present study, the anion resulting from the addition of an electron has been trapped in an X-irradiated crystal of 1,2-phenylenephosphorochloridite (**1**).

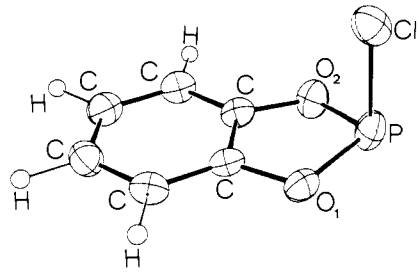

1

Information about the structure of this anion is obtained by examining the ESR tensors, the crystal structure of the host matrix, and the results of ab initio and INDO calculations. We will show that, in contrast with $PCl_3^{\bullet -}$ which adopts a T-shape structure, $PH_2Cl^{\bullet -}$ and $\mathbf{1}^{\bullet -}$ are pyramidal and bear their unpaired electron in a P–Cl σ^*-orbital. The dissociative energy of $PH_2Cl^{\bullet -}$ into $\dot{P}H_2 + Cl^-$ is calculated to be rather low and agrees with the thermal transformation of $\mathbf{1}^{\bullet -}$ into $C_6H_4O_2\dot{P}$ which is experimentally observed by ESR.

Experimental Section

Compounds and Crystal Mountings. 1,2-Phenylenephosphorochloridite was purchased from Aldrich. Single crystals have been obtained by melting the compound at 40 °C in a sealed vial and by decreasing the temperature very slowly to 77 K. The vial was then broken at 0 °C under an argon atmosphere, and one small fragment (~0.3 × 0.3 × 0.5 mm) was mounted in a Lindemann capillary and used for the X-ray diffraction study. Another fragment, of larger size (~2 × 3 × 3 mm), was rapidly glued on a small brass cube, at 10 °C under an argon atmosphere, and X-irradiated inside liquid nitrogen (irradiation conditions: 3 h, 30 kV, 30 mA Philips tube PW 1100 equipped with a tungsten anticathode). The properties of the compound (toxicity, melting point near room temperature, very hygroscopic) made all these manipulations very difficult, and we were compelled to use an arbitrary ESR reference frame.

Table I. Fractional Coordinates and Equivalent Isotropic Temperature Factors for $C_6H_4O_2PCl$[a]

	x	y	z	U_{eq}
Cl	0.40962 (15)	0.15743 (7)	0.03471 (9)	43.36 (23)
P	0.22495 (16)	0.27321 (8)	-0.08500 (8)	39.44 (24)
O(1)	-0.0200 (4)	0.27296 (21)	-0.00847 (21)	36.2 (6)
O(2)	0.3187 (4)	0.38820 (21)	-0.01472 (21)	39.4 (7)
C(1)	-0.0088 (5)	0.3477 (3)	0.0972 (3)	29.7 (7)
C(2)	-0.1681 (5)	0.3592 (3)	0.1939 (3)	36.2 (8)
C(3)	-0.1243 (6)	0.4413 (3)	0.2895 (3)	37.9 (9)
C(4)	0.0719 (6)	0.5078 (3)	0.2859 (3)	37.9 (9)
C(5)	0.2318 (6)	0.4950 (3)	0.1873 (3)	35.0 (8)
C(6)	0.1870 (5)	0.41401 (23)	0.0934 (3)	30.2 (7)

[a] Isotropic temperature factors, U_{eq} (Å^2 × 10^3), with esd's in parentheses. (U_{eq} is the average of the eigenvalues of U).

ESR Measurements. The ESR spectra were recorded on a Bruker ER 200 D spectrometer (X-band, 100 kHz field modulation). The klystron frequency was measured with a Hewlett Packard 5342A microwave frequency counter. Variable-temperature experiments were performed by using the Bruker 4111 accessory (temperature range 100–300 K). The temperature dependence of the ESR spectra was studied by warming the crystal and by recording the spectra at some selected temperatures. Each spectrum was obtained after stabilization of the temperature. The angular variations of the ESR signals were obtaind at 77 K by positioning the crystal in a finger Dewar and by rotating the sample in three per-

[†] Department de Chimie Physique.
[‡] Laboratoire de Chimie Théorique Appliquée.
[⊥] Laboratoire de Cristallographie aux Rayons X.

(1) (a) Gillbro, T.; Williams, F. *J. Am. Chem. Soc.* **1974**, *96*, 5032. (b) Hamerlinck, J. H. H.; Schipper, P.; Buck, H. M. *J. Am. Chem. Soc.* **1983**, *105*, 385. (c) Berclaz, T.; Geoffroy, M.; Lucken, E. A. C. *Chem. Phys. Lett.* **1975**, *36*, 677. (d) Nakanishi, A.; Nishikida, K.; Bentrude, W. *J. Am. Chem. Soc.* **1978**, *100*, 6398.

(2) (a) Morton, J. R.; Preston, K. F.; Strach, S. J. *J. Magn. Reson.* **1980**, *37*, 321. (b) Mishra, S. P.; Symons, M. C. R. *J. Chem. Soc., Dalton Trans* **1976**, 139.

(3) Janssen, R. A. J.; Visser, G. J.; Buck, H. M. *J. Am. Chem. Soc.* **1984**, *106*, 3429.

(4) Krusic, P. J.; Meakin, P. *Chem. Phys. Lett.* **1973**, *18*, 347.

(5) Hudson, A.; Whiffen, J. T. *Chem. Phys. Lett.* **1974**, *29*, 113.

(6) Hudson, R. L.; Williams, F. *J. Chem. Soc., Chem. Commun.* **1979**, 1125.

(7) Subramanian, S.; Rogers, M. T. *J. Chem. Phys.* **1972**, *57*, 4582.

(8) Morton, J. R.; Preston, K. F.; Strach, S. J. *J. Chem. Phys.* **1978**, *69*, 1392.

(9) (a) Geoffroy, M. *J. Chem. Phys.* **1979**, *70*, 1497. (b) Franzi, F.; Geoffroy, M.; Ginet, L.; Leray, N. *J. Phys. Chem.* **1979**, *83*, 2898.

0002-7863/86/1508-7148$01.50/0

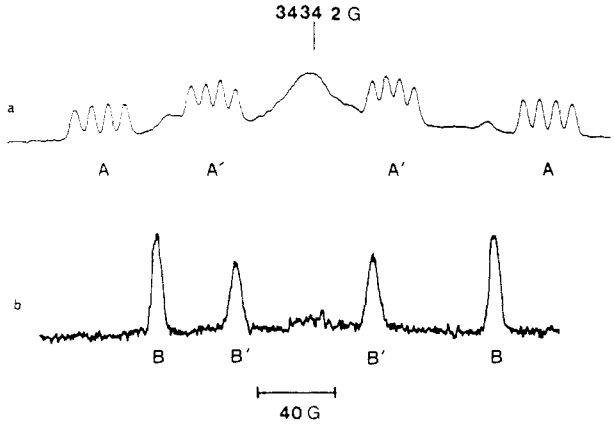

Figure 1. Second-derivative ESR spectra obtained with a crystal of **1** X-irradiated at 77 K: (a) spectrum obtained at 77 K without any annealing (A and A′ are attributed to $\mathbf{1}^{\bullet-}$ (two sites) and (b) after annealing at 245 K (B and B′ are attributed to **2** (two sites).

pendicular planes. The spectra were recorded every 10 deg. The corresponding experimental curves were analyzed with second-order perturbation by using a Hamiltonian which takes the Zeeman electronic effect and the various hyperfine interactions into account.

Crystallographic Data. The lattice parameters and intensities were measured at 200 K on a Philips PW 1100 diffractometer with graphite monochromated Mo Kα radiation. Monoclinic, $P2_1/c$, a = 5.8058 (11) Å, b = 12.029 (3) Å, c = 10.054 (2) Å, β = 92.04 (1)°, V = 701.7 Å^3, Z = 4; D_c = 1.652 g·cm^{-3}, Mo Kα, λ = 0.71069 Å, μ = 6.941 cm^{-1}, F_{000} = 352, cell dimensions from 23 reflections (2θ = 32–48°); data collection, $\sin\theta/\lambda \leq 0.62$, $\omega/2\theta$ scans, ω-scan angle 1.3°, no absorption correction, 2 standard reflections varied by a maximum of 3%, 1379 independent reflections, 757 observed reflections with $|F| \geq 3\sigma(F)$ and $|F| \geq 7$, distribution of data $\langle E^2 - 1 \rangle$ = 0.959 indicated centrosymmetric space group; structure solved by MULTAN 80;[10] full matrix least-squares with $|F|$ values; 91 parameters refined; no secondary-extinction corrections; all coordinates of the hydrogen atoms were calculated; R = 0.033, wR = 0.032 ($w = \exp[18(\sin\theta/\lambda)^2]$). Atomic scattering factors from *International Tables for X-Ray Crystallography*;[11] all calculations performed with local versions of XRAY76[12] and ORTEPII.[13] The fractional atomic coordinates are listed in Table I.

Calculations. All computations were performed on a VAX 11/780 computer. GAUSSIAN 80 and 82 versions[14] have been used for ab initio calculations. The optimized geometries for $PCl_3^{\bullet-}$, $H_2PCl^{\bullet-}$, and $\dot{P}H_2$ were obtained from UHF calculations (6-31G* basis set) by using gradient optimization techniques.[15,16] Hartree–Fock SCF and fourth-order Møller–Plesset (MP4)[17] calculations with the 6-31G* basis set were carried out for $H_2PCl^{\bullet-}$ and $H_2\dot{P}$. The spin densities for $PCl_3^{\bullet-}$, $H_2PCl^{\bullet-}$, and $\dot{P}H_2$ were obtained by using the UHF results for the optimized geometry, and additional ROHF calculations were performed in order to estimate the direction of the ^{31}P-hyperfine interaction tensor for $H_2PCl^{\bullet-}$ from the SOMO (singly occupied molecular orbital) coefficients.

Additional INDO calculations have been performed by using the parametrization of Oloff and Hüttermann.[18] Results for $H_2PCl^{\bullet-}$, $\dot{P}H_2$, and $PCl_3^{\bullet-}$ have been shown to be in good agreement with ab initio calculations; we have therefore used the INDO method for the radical species derived from the total molecule **1**.

Table II. Experimental ESR Tensors. Data in Parentheses Correspond to the Second Crystallographic Site

tensor	eigenvalues	eigenvectors x	y	z
		Radical A		
$\tilde{g}$	2.0054	0.202 (0.650)	0.504 (−0.108)	−0.839 (0.751)
	2.0023	−0.610 (0.749)	−0.605 (0.248)	−0.511 (−0.613)
	1.9942	−0.765 (−0.120)	0.615 (0.962)	0.185 (0.242)
^{31}P-$\tilde{T}$	868	0.459 (0.724)	0.537 (0.123)	0.707 (−0.678)
(MHz)	56	−0.159 (0.552)	0.833 (0.484)	−0.529 (0.678)
	44	−0.873 (0.412)	0.130 (−0.865)	0.468 (0.282)
^{35}Cl-$\tilde{T}$	41	0.036 (0.644)	0.692 (−0.317)	0.720 (−0.695)
(MHz)	20	−0.507 (−0.543)	−0.608 (0.450)	0.610 (−0.708)
	19	0.860 (0.538)	−0.387 (0.834)	0.329 (0.117)
		Radical B		
$\tilde{g}$	2.0052	0.385 (0.728)	−0.317 (0.692)	−0.695 (0.720)
	2.0022	0.331 (−0.683)	0.620 (0.025)	0.710 (0.729)
	1.996	0.860 (−0.046)	−0.507 (−0.998)	0.040 (−0.009)
^{31}P-$\tilde{T}$	755	0.304 (0.732)	0.663 (−0.068)	0.681 (−0.676)
(MHz)	111	−0.741 (0.514)	0.616 (0.706)	−0.265 (0.485)
	93	−0.596 (0.445)	−0.423 (−0.704)	0.681 (0.552)

Table III. Isotropic and Anisotropic Hyperfine Coupling Constants (MHz) and Corresponding Spin Densities Obtained by Using the Atomic Parameters Given by Morton and Preston[19]

	anisotropic coupling A_{iso}	τ	$\tau_{\perp_1}$	$\tau_{\perp_2}$	spin densities c_s^2	c_p^2
			Radical A			
^{31}P	322	545	−267	−278	0.02	0.74
^{35}Cl	26[a]	14	−6.5	−7.5	0.00	0.03
	0[b]	40	−20.5	−19.5	0.00	0.11
			Radical B			
^{31}P	319	435	−208.5	−226.5	0.02	0.59

[a] $T_\parallel > 0$, $T_\perp > 0$. [b] $T_\parallel > 0$, $T_\perp < 0$.

Results

ESR Spectroscopy. An example of an ESR spectrum recorded at 77 K, immediately after X-irradiation of a crystal of **1**, at 77 K, is shown in Figure 1a: besides a rather broad central line, eight signals, marked A, are observed. These signals are clearly due to a radical which exhibits hyperfine interaction with both a ^{31}P and a ^{35}Cl isotope. For some orientations of the magnetic field, lines due to ^{37}Cl are also detected. The angular dependence of these signals (Figure 2) shows that, in accord with the crystal structure, two sites are present and leads to the tensors given in Table II.

The temperature dependence of the spectrum (Figure 3) shows that above 200 K signals A are replaced by signals marked B on Figure 1b. Such a modification of the spectrum is consistent with the thermal transformation of the radical A into a new species B.

This species B exhibits a hyperfine coupling with a ^{31}P nucleus and the corresponding angular variation is shown in Figure 4. These curves lead to the ESR tensors given in Table II.

The various hyperfine coupling tensors obtained for species A and B have been decomposed into isotropic and anisotropic coupling constants. Comparison of these values with the atomic parameters compiled by Morton and Preston[19] leads to the experimental spin densities given in Table III; for the chlorine coupling two possible sign combinations have been considered: $T_\parallel > 0$, $T_\perp > 0$ and $T_\parallel > 0$, $T_\perp < 0$.

Theoretical Results. Preliminary Calculations. In order to estimate the reliability of our ab initio calculations, we have determined the optimized structures of H_2PCl and $PCl_3^{\bullet-}$.

(10) Main, P.; Fiske, S. J.; Hull, S. E.; Lessinger, L.; Germain, G.; Declercq, J. P.; Woolfson, M. M. A System of Computer Programs for the Automatic Solution of Crystal Structures from X-Ray Diffraction Data; Universities of York and Louvain-la-Neuve; 1980.
(11) *International Tables for X-Ray Crystallography*; Kynoch Press: Birmingham, 1974; Vol. IV.
(12) Stewart, J. M.; Machin, P. A.; Dickinson, C. W.; Ammon, H. L.; Flack, H. The X-Ray'76 System. Technical Report TR 446. Computer Science Center, University of Maryland: College Park, Maryland.
(13) Johnson, C. K. ORTEP II. Report ORNL-5138. Oak Ridge National Laboratory, 1976.
(14) (a) Binkley, J. S.; Whiteside, R. A.; Krishnan, R.; Seeger, R.; De Frees, D. J.; Schlegel, H. B.; Topiol, S.; Kahn, L. R.; Pople, J. A. *QCPE* **1981**, *13*, 406. (b) Binkley, J. S.; Frisch, M. J.; De Frees, D. J.; Raghavachari, K.; Whiteside, R. A.; Schlegel, H. B.; Fluder, E. M.; Pople, J. A. GAUSSIAN 82, Carnegie-Mellon University: Pittsburgh, 1983.
(15) Binkley, J. S. *J. Chem. Phys.* **1976**, *64*, 5143.
(16) Fletcher, R.; Powell, M. J. D. *Comput. J.* **1973**, *6*, 163.
(17) (a) Pople, J. A.; Binkley, J. S.; Seeger, R. *Int. J. Quantum Chem., Symp.* **1976**, *10*, 1. (b) Krishnan, R.; Pople, J. A. *Int. J. Quantum Chem.* **1976**, *14*, 91.
(18) Oloff, H.; Hüttermann, J. *J. Magn. Reson.* **1980**, *40*, 415.
(19) Morton, J. R.; Preston, K. F. *J. Magn. Reson.* **1978**, *30*, 577.

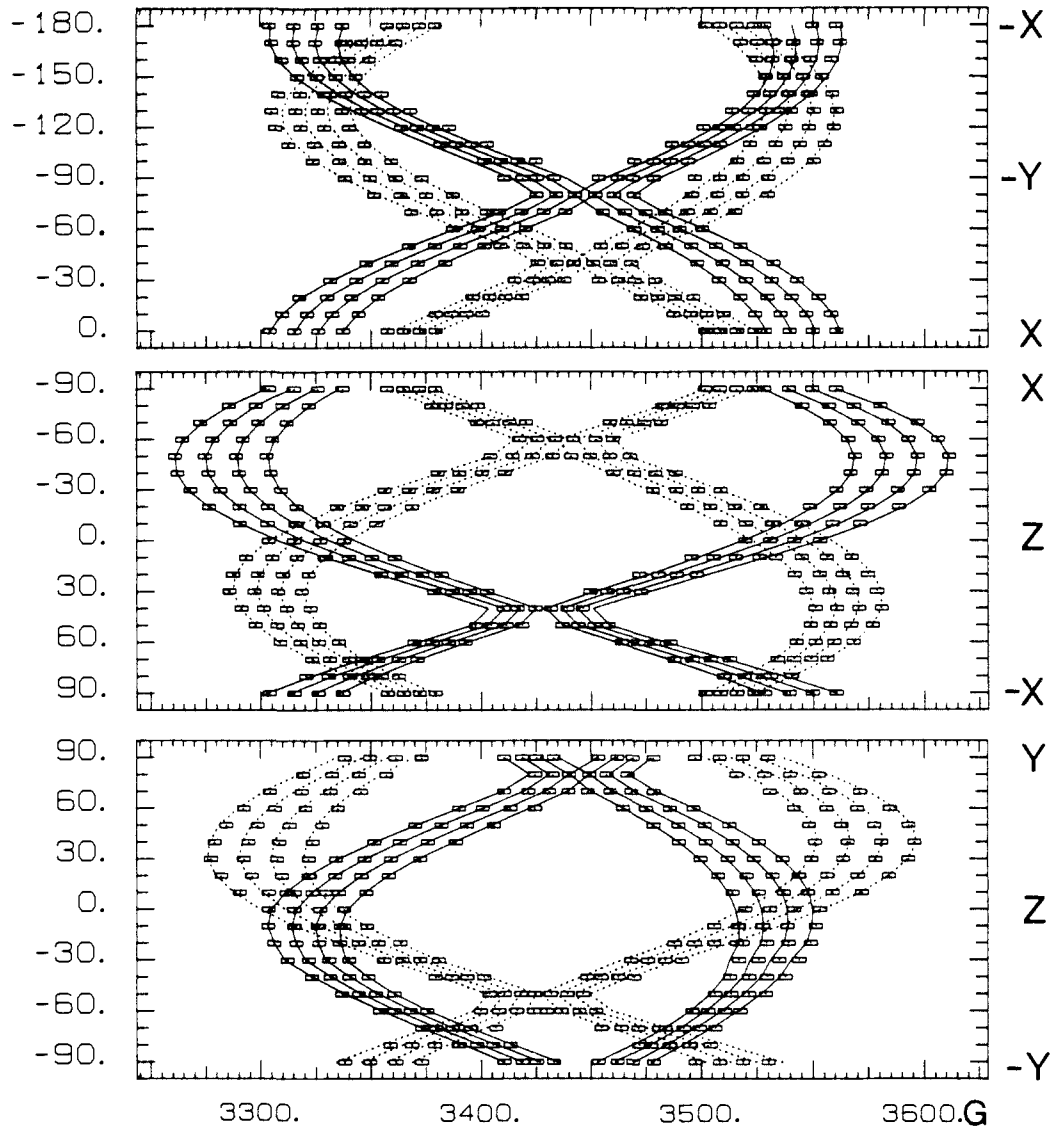

Figure 2. Angular dependence of signals of signals A and A'.

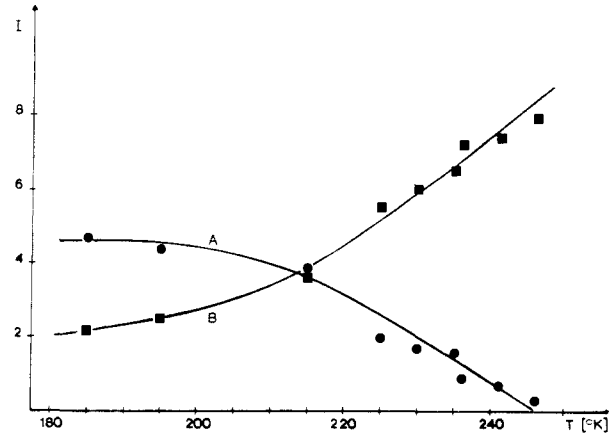

Figure 3. Temperature dependence of the intensity (in arbitrary units) of signals A and B.

(a) H_2PCl. The geometry was optimized by assuming equal PH bond lengths. The final structure is shown in Figure 5a ($E_{tot.}$[RHF] = -801.368 87 au); the optimized parameters are consistent with the experimental structure obtained for F_2PH by microwave spectroscopy[20] (PF = 1.58 Å, PH = 1.41 Å, HPF = 96.3°, FPF = 99.0°). They are in very good accord with the crystal structure determined for **1**: P–Cl = 2.108 Å, P–O_1 = 1.640 Å, P–O_2 = 1.637 Å, ClPO_1 = 99.3°, ClPO_2 = 99.0°, OPO = 94.5°, Φ = 13.3°.

(b) $PCl_3^{\bullet-}$. The geometry was optimized by assuming that the PCl(3) bond lies in the bisector plane of the Cl(1)PCl(2) angle. The results are shown in Figure 5b ($E_{tot.}$[UHF] = -1 719.257 22 au). This geometry is very close to the T-shape structure predicted by Subramanian and Rogers[7] on the basis of their experimental results on $AsCl_3^{\bullet-}$ and of their CNDO calculations. Our ab initio calculations indicate that the major spin density is located in a phosphorus p-orbital oriented perpendicular to the molecular plane (Table IV).

Calculations of $H_2PCl^{\bullet-}$. Ab Initio: We have assumed that the two PH bonds have equal lengths and that the chlorine atom lies in the HPH bisector plane. UHF calculations at the SCF level lead to the following optimized geometry: P–H = 1.40 Å, P–Cl = 3.48 Å, HPH = 94.3°, HPCl = 72.4°. Inspection of the potential energy curve (Figure 6) indicates that this structure corresponds to a nearly dissociative state. In order to estimate the effect of electron correlation on this potential energy curve, we have performed additional MP4 calculations. The convergence of the optimization process was very slow, and when it appeared that the value of the HPH angle was not changing any more, we kept only the HPCl angle and the PCl distance as variable parameters. The final values are given in Figure 5c ($E_{tot.}$[UHF,MP4] = -801.636 63 au). It can be noted that the correlation effects considerably shorten the PCl distance (from 3.48 to 3.04 Å) and increase the HPCl angle (from 72.4° to 81°).

(20) Kruczkowski, R. L. *J. Am. Chem. Soc.* **1968**, *90*, 1705.

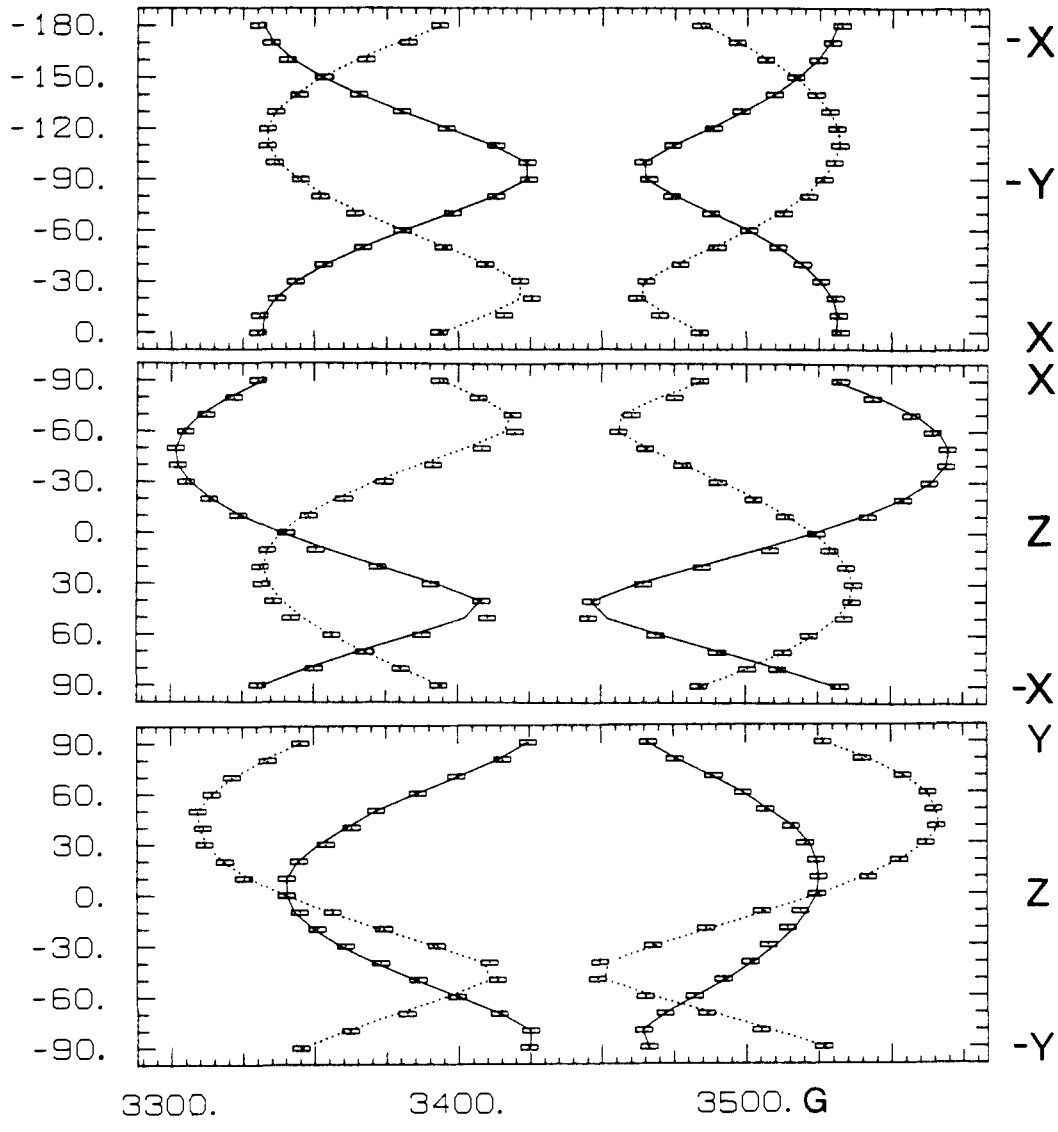

Figure 4. Angular dependence of signals B and B′.

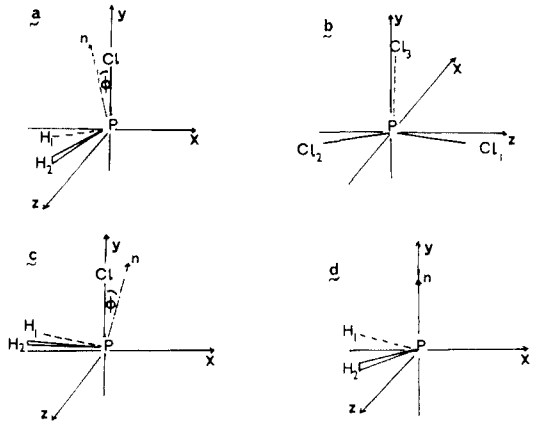

Figure 5. Optimized geometries for the following: (a) H_2PCl, HPCl = 97°4, HPH = 94°4, Φ = +11°, H–P = 1.39 Å, P–Cl = 2.07 Å; (b) $PCl_3^{\bullet-}$, Cl_1 and Cl_2 lie in the YOZ plane, Cl_3 is in the XOY plane, Cl_1PCl_2 = 173.4°, Cl_1PCl_3 = Cl_2PCl_3 = 93.3°, Cl_3PY = 0.3°, P–Cl_1 = P–Cl_2 = 2.44 Å, P–Cl_3 = 2.07 Å; (c) $H_2PCl^{\bullet-}$, HPH = 93°, H_1PCl = H_2PCl = 81°, Φ = −13°, P–H = 1.42 Å, P–Cl = 3.04 Å; (d) PH_2, HPH = 93.4°, P–H = 1.40 Å. For a, c, and d *n* is perpendicular to the HPH plane.

We have estimated the dissociation energy of $H_2PCl^{\bullet-}$ into $H_2\dot{P}$ and Cl^- by studying the variation of the potential energy surface as a function of the P–Cl distance. In this calculation all the geometrical parameters were kept constant (Figure 5c) except the P–Cl distance. The energy corresponding to d(P–Cl) = ∞ was obtained from separate calculations performed for the fragments $\dot{P}H_2$ and Cl^-. The optimized structure of the radical $\dot{P}H_2$ is given in Figure 5d (E_{tot}[UHF,MP4] −341.958 83 au). As shown in Figure 6, the dissociation energy ΔE for $PH_2Cl^{\bullet-}$ at (E_{tot}[UHF,MP4] = −341.958 83 MP4 level is equal to 7.3 kcal/mol (at the SCF level ΔE was found to be only 2.5 kcal/mol).

The energy levels shown in Figure 7 have been obtained from ROHF calculations performed on the optimized structure in Figure 5c. Clearly, it appears that the two chlorine p_x and p_z orbitals do not mix with any phosphorus orbital and that their energy levels lie between those of the P–Cl σ and σ* (SOMO).

The LCAO coefficients of the SOMO lead to the spin population given in Table IV. These spin densities are appreciably increased if the overlap contribution is taken into account (see the spin densities derived from gross orbital populations in Table IV).

INDO Results. The net spin densities predicted by the INDO model for the ab initio optimized structure of $H_2PCl^{\bullet-}$ are given in Table IV. The same calculations have been carried out for the anion $\mathbf{1}^{\bullet-}$, and in this case we have assumed that the geometry of the OP(O)Cl moiety is the same as the geometry optimized for the HP(H)Cl anion and that the other structural parameters are those obtained by crystallography for the neutral molecule. The corresponding spin densities are given in Table IV.

Discussion

Identification of the Phosphorochloridite Radical Anion $\mathbf{1}^{\bullet-}$. In order to facilitate the identification of radical A we will first

Table IV. Theoretical and Experimental Spin Densities

radical		spin densities: phosphorus 3s	3p$_x$	3p$_y$	3p$_z$	chlorine 3s	3p$_x$	3p$_y$	3p$_z$
$PCl_3^{\bullet-}$	a	0.06	0.92	−0.06	0.04	0.00	0.02	0.00	−0.02
						0.00	0.02	0.00	−0.02
						0.00	0.03	0.01	0.00
	b	0.01	0.86	0.00	0.02	0.00	0.02	0.00	0.01
						0.00	0.02	0.00	0.01
						0.00	0.08	0.01	0.00
$\dot{P}H_2$	a	0.09	−0.03	0.99	0.04				
	b	0.01	0.04	1.00	0.07				
		1s (H_1, H_2): −0.06							
2	b	0.01	0.01	0.77	0.02				
	d	0.02		0.59					
$H_2PCl^{\bullet-}$	a	0.09	0.07	0.81	0.04	0.00	0.00	0.07	0.00
	b	0.01	0.08	0.73	0.05	0.00	0.00	0.20	0.00
	c	0.04	0.07	0.59	0.00	0.01	0.00	0.08	0.00
1$^{\bullet-}$	b	0.01	0.10	0.63	0.02	0.00	0.00	0.12	0.00
	d	0.02		$c_p^2 = 0.74$		0.00		$c_p^2 = 0.11$	

[a] Spin densities derived from gross orbital population obtained from ab initio UHF calculations. Before annihilation of the first spin contaminant, the expectation values $\langle S^2 \rangle$ for $PCl_3^{\bullet-}$, $\dot{P}H_2$, and $H_2PCl^{\bullet-}$ are equal to 0.77, 0.76, and 0.76, respectively. [b] Net spin densities obtained from INDO calculations. [c] Net spin densities obtained from the LCAO coefficients of the SOMO (ROHF ab initio calculations). [d] Experimental spin densities obtained in the hypothesis of $^{31}P-T_{\parallel} > 0$, $^{31}P-T_{\perp} > 0$, $^{35}Cl-T_{\parallel} > 0$, $^{35}Cl-T_{\perp} < 0$.

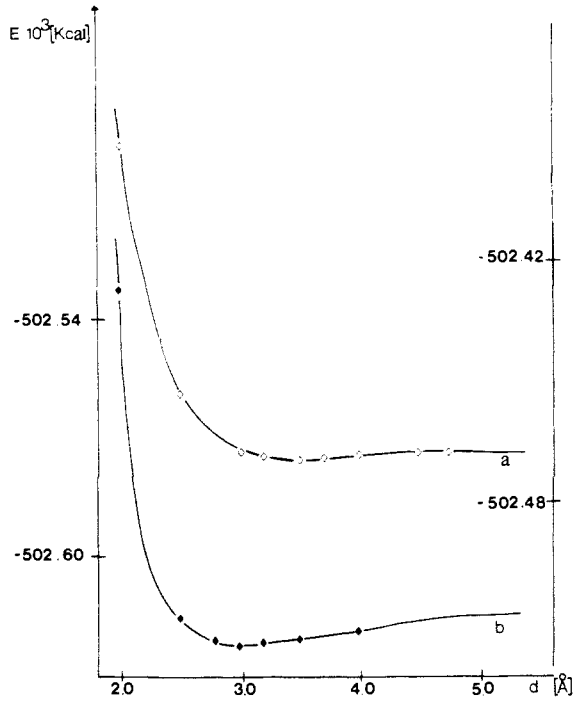

Figure 6. Potential energy curve for $H_2PCl^{\bullet-}$: (a) ab initio UHF calculations at the SCF level (energy scale on the right axis), (b) Fourth-order Møller–Plesset calculations (energy scale on the left axis).

examine the ESR results obtained for radical B.

Radical B. This radical exhibits hyperfine coupling with only a ^{31}P nucleus. Whatever the sign combination which is used in Table III, it is clear that the unpaired electron is mainly localized in a phosphorus 3p-orbital. The $^{31}P-T_{\parallel}$ direction is aligned along the eigenvector associated with g_2 ($\simeq$2.0023), as is expected for a phosphinyl type radical $R_2\dot{P}$.[21] For such a species the unpaired electron is indeed confined to a phosphorus p-orbital oriented

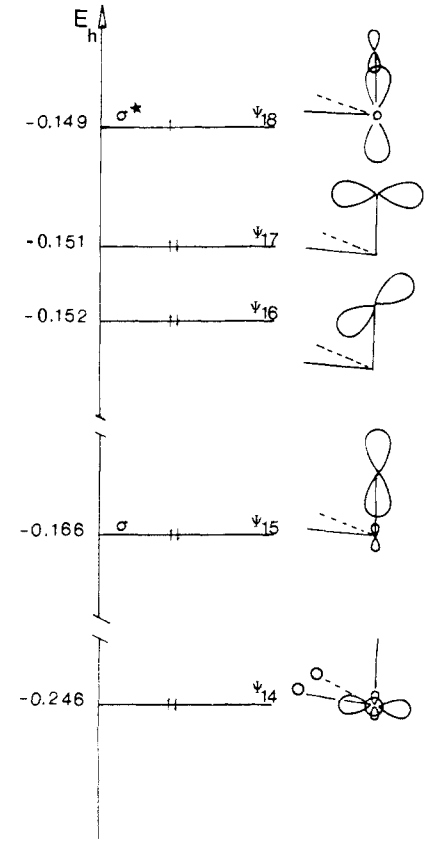

Figure 7. MO energy levels obtained from ROHF ab initio calculations for $H_2PCl^{\bullet-}$.

perpendicular to the RPR plane. This structure is confirmed by the ab initio results obtained for $H_2\dot{P}$ and by the INDO results obtained for **2** (Table IV).

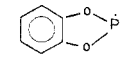

2

We have therefore identified the radical B to be the phosphinyl radical **2**. Furthermore, this conclusion is supported by the fact that the angle between the $^{31}P-T_{\parallel}$ direction of the two sites (θ_1 = 73°) is near that formed by the normals to the OPO planes measured on the undamaged molecule (θ_2 = 64°). The small difference ($\theta_1 - \theta_2$) may indicate a slight reorientation (4.5°) of the OPO plane accompanying the departure of chlorine.

Radical A. The experimental spin densities given in Table III show that the SOMO is essentially built from a phosphorus p-orbital and, to a much lesser extent, from a chlorine p-orbital. The very small isotropic coupling indicates that species A cannot be a phosphoranyl radical $\dot{P}R_4$,[1] nor an anion $PR_5^{\bullet-}$,[2] nor a cation $PR_3^{\bullet+}$.[22] Only two candidates need to be considered: the phosphinyl R$\dot{P}$Cl and the $R_2PCl^{\bullet-}$ anion. The data reported in Table II for radical A are not inconsistent with those recently reported by Bonazzola et al.[23] for $\dot{P}Cl_2$ and could suggest the scission of a O–P bond. However, we abandon this hypothesis for the following reasons: (i) The crystal structure shows that the Cl atom lies in the symmetry plane of **1**; the O(1)P and O(2)P have therefore the same probability to undergo a homolytic scission. Each rupture giving rise to two sites, we would detect more than two sites for some orientations of the magnetic field. (ii) The $^{35}Cl-T_{\parallel}$ direction has been shown to be aligned along the $^{31}P-T_{\parallel}$ direction for R$\dot{P}$Cl,[23] and in our case the angle between these two directions is actually equal to 26°. (iii) The experimentally observed transformation of radical A into the $R_2\dot{P}$ species

(21) Geoffroy, M.; Lucken, E. A. C.; Mazeline, C. *Mol. Phys.* **1975**, *29*, 839.

(22) Berclaz, T.; Geoffroy, M. *Mol. Phys.* **1975**, *30*, 549.

(23) Bonazzola, L.; Michaut, J. P.; Roncin, J. *J. Chem. Phys.* **1981**, *75*, 4829.

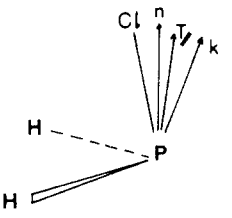

Figure 8. Theoretical mutual orientation of the various structure parameters for $H_2PCl^{\bullet-}$. n is normal to the HPH plane, k is the direction of the P–Cl bond in neutral HPCl, $T_\parallel$ is the direction of the hyperfine eigenvector; $^{31}P\text{–}T_\parallel$, (P–Cl,$n$) = 11°, ($k$,$n$) = −13°, (P–Cl,$T_\parallel$) = 19°, ($T_\parallel$,$k$) = 5°.

is the expected result of thermal decomposition of an $R_2PCl^{\bullet-}$ anion.

Structure of $R_2PCl^{\bullet-}$. In accordance with the theoretical results found for $H_2PCl^{\bullet-}$ (ab initio and INDO) and $\mathbf{1}^{\bullet-}$ (INDO) the experimental hyperfine tensors measured for radical A indicate that the unpaired electron mainly occupies a phosphorus p-orbital and is very slightly delocalized in a Cl p-orbital. The combination $^{35}Cl\text{–}T_\parallel > 0$, $^{35}Cl\text{–}T_\perp < 0$ leads to excellent agreement between the experimental chlorine spin densities and the INDO values. In contrast with $PCl_3^{\bullet-}$, the results given in Figure 5 show that the most stable structure for $H_2PCl^{\bullet-}$ is not the planar T-shape but a pyramid with an elongated P–Cl bond. Another striking feature for $H_2PCl^{\bullet-}$ is the value of the Φ angle formed by the normal to the HPH plane and the P–Cl bond. This angle is negative for the anion (Φ = −13°) and positive for the neutral molecule (Φ = +11°).

As indicated by ab initio and INDO calculations, the hyperfine interaction with ^{35}Cl is only due to some spin density in the Cl p_y orbital; the $^{35}Cl\text{–}T_\parallel$ eigenvector is therefore aligned along the P–Cl bond of $H_2PCl^{\bullet-}$. The various atomic contributions to the SOMO show that, for the phosphorus atom, the spin resides in both the p_y (ρ_y = 58%) and the p_x (ρ_x = 7%) orbitals. the $^{31}P\text{–}T_\parallel$ eigenvector is therefore expected to make an angle of ~20°[24] with the Y axis (the P–Cl bond direction), implying that the $^{31}P\text{–}T_\parallel$ direction must approach the P–Cl direction of the neutral molecule.

These angular properties are quite consistent with the experimental eigenvectors reported in Table II: ($^{31}P\text{–}T_\parallel$, $^{35}Cl\text{–}T_\parallel$) = 26°, and the angle ($^{31}P\text{–}T_{\parallel site1}$, $^{31}P\text{–}T_{\parallel site2}$) is equal to 85° while the crystallographic angle ($P\text{–}Cl_{site1}$, $P\text{–}Cl_{site2}$) is equal to 84°.

Dissociation of the Radical Anion. The dissociation energy of $H_2PCl^{\bullet-}$ calculated by ab initio is small (ΔE = 7 kcal/mol), and it is possible that, in our experiment, the crystal matrix participates in the stabilization of $\mathbf{1}^{\bullet-}$. As shown in Figure 5 electron capture by R_2PCl gives rise to an increase of the P–Cl bond length which passes from 2.0 to 3.0 Å. This electron addition can be compared with that observed for the carbon halides;[25] whereas CF_3Br gives rise to $CF_3Br^{\bullet-}$,[26] ESR studies have shown that the adduct $\dot{C}H_3\cdots Br^-$ is the species produced in irradiated CH_3Br.[27] The halogen spin density calculated for $\mathbf{1}^{\bullet-}$ or deduced from experimental measurements (in the hypothesis of $T_\parallel > 0$, $T_\perp < 0$) is, in fact, nearer that found for the real anion $CH_3X^{\bullet-}$ than that observed for the adduct $\dot{C}H_3\cdots X^-$.

Conclusion

The calculations have shown that the geometry of $PCl_3^{\bullet-}$ corresponds to an almost planar T-shape structure while $H_2PCl^{\bullet-}$ adopts a pyramidal structure for which the unpaired electron occupies a P–Cl σ^* orbital. The calculated dissociation energy for $H_2PCl^{\bullet-}$ is rather low and explains why the anions resulting from the electron capture by a trivalent phosphorus are practically never observed. The experimental ESR parameters found after irradiation of **1**, at low temperature, are in good accord with the theoretical results obtained for $R_2PCl^{\bullet-}$ and it is possible that some matrix effects help in the stabilization of $\mathbf{1}^{\bullet-}$.

Acknowledgment. The financial support of the Swiss National Science Foundation is gratefully acknowledged.

Supplementary Material Available: Tables of bond lengths and angles and anisotropic displacement parameters along with a computer generated plot (7 pages); tables of structure factors (23 pages). Ordering information is given on any current masthead page.

(24) The hyperfine eigenvectors associated with the spin distribution c_y^2 and c_x^2 are obtained by calculating $\langle c_y p_y + c_x p_x | T | c_y p_y + c_x p_x \rangle$, where T is the dipolar hyperfine operator. These integrals can be evaluated by using the program QCPE 145 (Kern, C. W.; Karplus, M. *J. Chem. Phys.* **1965**, *43*, 415) or by using the results mentioned in the following: Franzi, R.; Geoffroy, M.; Lucken, E. A. C.; Leray, N. *J. Chem. Phys.* **1983**, *78*, 708.

(25) Wang, J. T.; Williams, F. *J. Am. Chem. Soc.* **1980**, *102*, 2860.
(26) Hasegawa, A.; Williams, F. *Chem. Phys. Lett.* **1977**, *46*, 66.
(27) Sprague, E. D.; Williams, F. J. *Chem. Phys.* **1971**, *54*, 5425.